Polymer Chemistry

RSC Publishing

COMMUNICATION

View Article Online
View Journal | View Issue

Autonomous self-healing of poly(acrylic acid) hydrogels induced by the migration of ferric ions†

Cite this: *Polym. Chem.*, 2013, **4**, 4601

Zengjiang Wei,[ab] Jie He,[b] Tony Liang,[b] Hyuntaek Oh,[c] Jasmin Athas,[b] Zhen Tong,[a] Chaoyang Wang*[a] and Zhihong Nie*[b]

Received 28th May 2013
Accepted 16th June 2013

DOI: 10.1039/c3py00692a

www.rsc.org/polymers

A facile and versatile strategy was developed for the preparation of self-healing hydrogels containing double networks of both physically and chemically cross-linked polymers. The autonomous self-healing of the hydrogel was achieved through the dynamic bonding of physical cross-linking and the migration of ferric ions.

Hydrogels are physically and/or chemically cross-linked networks of hydrophilic polymer chains.[1] They have shown an enormous amount of attractive applications, such as in biosensors,[2] drug delivery,[3–7] soft robots,[8,9] and scaffolds for cell and tissue culture.[10] Particularly, hydrogels that are capable of repairing themselves after damage represent a new class of "intelligent" materials that can actively adapt to their surroundings. These hydrogel materials have attracted considerable attention due to their self-healing nature and resulting applications, such as in tissue engineering.[11–13]

Recently, great progress has been made in the development of stimuli-responsive self-healing materials capable of responding to external triggers such as pH,[14–16] light,[17] electricity,[18] and redox potential.[3,19] The self-healing of hydrogels is mostly achieved by reversible interactions between polymer backbones and/or functional groups of polymers within the hydrogels. Typical interactions include supra-molecular interactions,[15] host–guest interactions,[14,19,20] freezing–thawing systems,[21] dynamic covalent bonding,[22] hydrogen bonding,[23,24] and ionic bonding of polymer chains and Ca^{2+} ions.[25] However, these self-healing systems usually either require sophisticated synthesis of the polymers, or need the encapsulation of healing agents[26] or the variation in the ambient conditions, *i.e.* pH,[23,24] temperature, electricity, electromagnetic wave, IR light,[18] or ionic strength.[27,28]

Herein, we report a simple yet versatile approach to design autonomous self-healing hydrogels without the need of human intervention or external energy. The self-healing system comprises of both ionically and covalently cross-linked networks of polymer chains. The covalent cross-linking of polymers provides a mechanical support to sustain the shape of the hydrogels. The mobility of free ferric ions and the dynamic ionic bonding in the hydrogels enables the rapid reversible cross-linking of polymer chains in the damaged region for the self-healing. The self-healing efficiency of the hydrogels is largely dependent on the concentration of ferric ions and the mobility of the uncross-linked segments of polymer chains.

The self-healing hydrogels were prepared *via* free radical polymerization of acrylic acid (AA) in the presence of *N*,*N*′-methylene-bis-acrylamide (MBAA, chemical cross-linker) and $FeCl_3$ (see the detailed experimental procedures in the Electronic Supplementary Information, ESI, and the schematic of this polymerization in Fig. S1a†). The polymerization produced chemically cross-linked PAA chains to maintain a permanent hydrogel network, while the ionic bonding between ferric ions and carboxylic groups acted as a physical cross-link to form secondary networks within the hydrogels (Fig. 1a). The hydrogels with various compositions, listed in Table 1, were prepared and investigated. The representative hydrogel (Entry 3) was prepared by a recipe containing 1.39 mol L^{-1} of AA, 1.25% $FeCl_3$ (mol%, $FeCl_3$/AA) and 0.1% MBAA (mol%, MBAA/AA).

All hydrogel samples were fabricated into a cylindrical shape with a diameter of 1 cm in order to study their self-healing behavior. The hydrogel (Table 1, Entry 3) was cut into two halves. The two halves self-healed when they were brought into contact and left undisturbed at room temperature for approximately 6 hours (Fig. 1b–e). After the healing, no obvious vestige of the physical damage was observed at the junction. The self-healed hydrogel could withstand stretching up to ~200% of its original length before the appearance of mechanical failure

[a]*Research Institute of Materials Science, South China University of Technology, Guangzhou 510640, China. E-mail: zhywang@scut.edu.cn*

[b]*Department of Chemistry and Biochemistry, University of Maryland, College Park, MD 20742, USA. E-mail: znie@umd.edu*

[c]*Department of Chemical and Biomolecular Engineering, University of Maryland, College Park, MD 20742, USA*

† Electronic supplementary information (ESI) available: The synthetic and self-healing experimental details, Raman, FTIR, and self-healing coatings. See DOI: 10.1039/c3py00692a

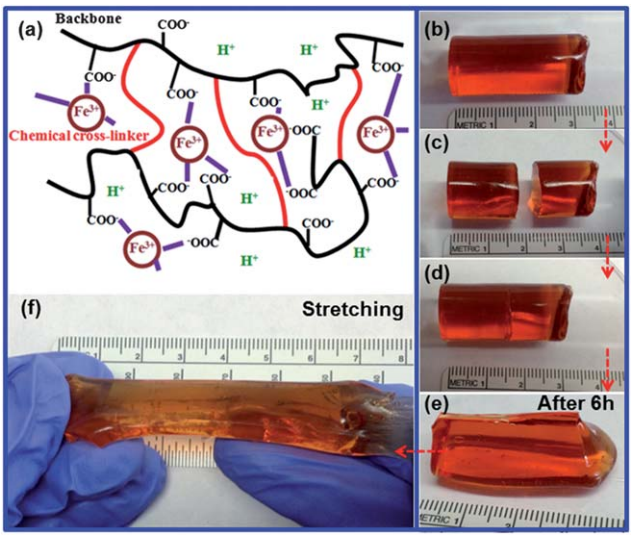

Fig. 1 (a) Schematic illustration of the structure of the self healing hydrogel. (b)–(e) Self healing of a cylindrical hydrogel (Entry 3) at room temperature: (b) the original hydrogel, (c) the hydrogel after being cut, (d) the hydrogel after the two parts were brought into contact with each other, (e) the hydrogel after healing for 6 hours. (f) Stretching the self-healed hydrogel up to ~200%.

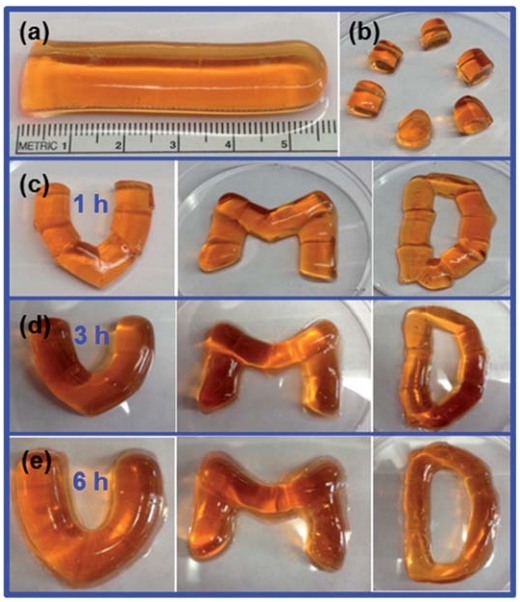

Fig. 2 The use of the self-healing nature of the hydrogel to produce complex architectures. (a) The original hydrogel. (b) The hydrogel after being cut. (c–e) The hydrogel segments arranged in the form of letters: U, M, and D, after (c) 1 hour, (d) 3 hours, and (e) 6 hours of self-healing.

Table 1 Hydrogels with various compositions

Entry	AA (g)	Water (g)	Fe^{3+}/AA (mol%)	$(NH_4)_2S_2O_8$ (g)	MBAA/AA (mol%)
1	1	9	0	0.05	0.1
2	1	9	0.5	0.05	0.1
3	1	9	1.25	0.05	0.1
4	1	9	2.5	0.05	0.1
5	1	9	1.25	0.05	0
6	1	9	2.5	0.05	0
7	1	9	1.25	0.05	0.25
8	1	9	1.25	0.05	0.5
9	1	9	1.25	0.05	1
10	1	9	0	0.05	1

(Fig. 1f). When the hydrogel (Entry 3) was cut into multiple pieces it still displayed efficient self-healing after 6 hours (Fig. S2a–e†), and the healed gel could be stretched up to ~200% of its original length (Fig. S2e and f†). The self-healing process was repeatable, and the hydrogel did not show any obvious decay of its mechanical properties after six healing cycles. More complex architectures of hydrogels could be produced through the healing of multiple pieces (Fig. 2). The ability of fusing multiple hydrogel pieces may enable the development of structured soft materials with complex architectures with potential applications in soft actuators or robotic devices.

The hydrogel networks consist of two types of interactions, that is, covalent bonds and ionic interactions. The self-healing of the hydrogel is driven by the dynamic ionic bonding between ferric ions and carboxylic groups of PAA. On one hand, the presence of a small amount of a chemical cross-linker (~5 mol%, MBAA/AA) led to the formation of the mechanically strengthened hydrogels with inter-chain chemical cross-linking and intramolecular hydrogel bonding of PAA chains. On the other hand, the multiple ionic interactions between Fe^{3+} ions and carboxy groups of PAA produced a non-covalent network of polymer chains.[29] The dynamic nature of ionic interactions plays a critical role in self-healing. The Fe^{3+} ions diffuse towards the freshly cut interface and interact with carboxy groups of PAA chains with the assistance of the mobility of the PAA chain segments. The formation of inter-chain bonding between PAA and Fe^{3+} ions across the interface repairs the damage and rejoins the two pieces of gel. Since the self-healing process only reforms the non-covalent network rather than the covalent network, the self-healing would compromise the mechanical strength of the hydrogels to a certain extent.

The properties of the sample of Entry 3 were examined by dynamic rheology measurements. A strain amplitude sweep measurement was performed to analyze the storage modulus G' and the loss modulus G'' of this gel as a function of the oscillatory strain amplitude, γ_0 (Fig. 3a). When $\gamma_0 < 420\%$, the hydrogel showed elastic features, as indicated by the constant value of both G' and G'', and $G' > G''$. When $\gamma_0 > 420\%$, the G' value decreased rapidly and G'' approached the value of G', indicating the collapse of the gel network.[23] A frequency sweep measurement was also performed to confirm the gel-like behavior of this hydrogel. As shown in Fig. 3b, G' is larger than the G'' in the range of all the frequencies studied, and both moduli show weak dependency on the angular frequency ω at frequencies greater than 0.01 rad per s. Crossover of G' and G'' occurs at a frequency of approximately 0.01 rad per s, indicating that the relaxation time, t_R, of this gel is more than 100 seconds. This value of t_R is large enough for practical applications of this hydrogel, compared to self-healing hydrogels reported previously.[22]

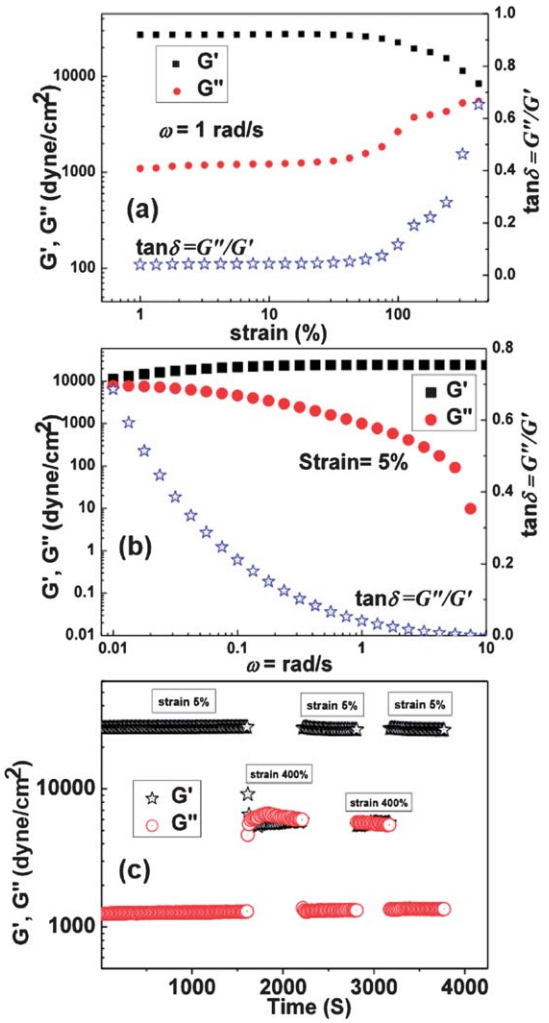

Fig. 3 Rheology test of this self-healing hydrogel. (a) Storage moduli G' and loss moduli G'' as a function of strain in a strain amplitude sweep test. (b) Frequency sweep test of the hydrogel. (c) G' and G'' from continuous strain sweep with the hydrogel alternatively subjected to a small oscillation force (5% strain) and a large oscillation force (400% strain).

Rheological characterization was also carried out to further demonstrate the robust self-healing properties of this hydrogel. Fig. 3c demonstrates the repeated recovery of the gel's properties following disruptive mechanical shearing forces. Initially, the hydrogel (Entry 3) was subjected to a small amplitude oscillatory shear (strain = 5% at frequency = 1 rad per s) for 1600 s. At this condition, G' is greater than G'', and both moduli do not change with time. This implies that the hydrogel network remains intact under small oscillatory strain. Afterwards, the hydrogel was subjected to a large amplitude oscillatory shear (strain = 400% at a frequency of 1 rad per s) for 600 s. During this process, the G' value decreased drastically from ~27 k to ~6 k dyne per cm^2. The value of G' is close to that of G'', indicating the rupture of the gel network. Subsequently, the hydrogel was subjected to a low amplitude strain of 5%, which is within the constant regime in Fig. 3a. The gel-like character ($G' > G''$) was recovered instantaneously, and G' and G'' recovered to the initial values immediately. This indicates the complete recovery of the hydrogel network after disruption, confirming the self-healing capability of the hydrogel. This disruption and recovery of the gel properties under different oscillatory shears can be repeated several times (Fig. 3c).

In order to elucidate the underlying mechanism of the self-healing, we systematically studied the effect of various parameters, including the concentration of Fe^{3+} ions, density of chemical cross-linking, and healing time. The strength of the hydrogel is denoted by its maximum strain (ε), which is determined by $\varepsilon = L/L_0 \times 100\%$, where L is the stretched length at break and L_0 is the original length. To quantify the self-healing properties of the hydrogel, the healing efficiency (f) is defined as $f = \varepsilon'/\varepsilon$, where ε' is the strain of the healed hydrogel and ε is the strain of the original hydrogel (uncut hydrogel). The closer the value of f to 1, the more desirable the self-healing capability is, whereas a value that is closer to zero indicates a less efficient self-healing.

First, we varied the concentration of $FeCl_3$ during the preparation of the hydrogel (Table 1). The concentration of Fe^{3+} ions plays a critical role in the self-healing efficiency of the gel (Fig. 4a). In the absence of $FeCl_3$, the hydrogel (Entry 1) did not self-heal despite a prolonged contact time between the gel pieces ($\varepsilon' = \sim 125\%$, $f = \sim 0.2$). Upon the addition of $FeCl_3$, the ε' of healed gels significantly increased. A healed hydrogel (Entry 3) composed of 1.25 mol% of $FeCl_3$ exhibited an ε' value of ~286% and an f value of ~0.88. This indicates that the diffusion of Fe^{3+} ions led to the cross-linking of polymer networks at the interface, thus the healing of the hydrogel. The self-healing efficiency remained stable with further increasing the concentration of $FeCl_3$, while sacrificing the ε of the hydrogel. For example, when the concentration of Fe^{3+} ions was 2.5%, the ε of the hydrogel was 174%, which was approximately half of the ε of 324% for the hydrogel with 1.25% $FeCl_3$, despite the high self-healing efficiency (f) of ~0.7. This indicates that the high physical cross-linking density of polymers hinders the stretching of hydrogels, that is, a decrease in the elastic properties of the hydrogel, ε. We found that an Fe^{3+} concentration of 1.25% offers the hydrogel optimal elastic properties and healing efficiency.

Next, we evaluated the effect of the chemical cross-linking density on the self-healing efficiency by varying the concentration of the chemical cross-linker, [MBAA] (Table 1). An increase of [MBAA] led to a rapid decrease in the value of ε' and f (Fig. 4b). 0.5–1 mol% of MBAA led to an almost complete loss of the self-healing properties of the hydrogel. When [MBAA] was less than 0.1 mol%, the ε' of the self-healed hydrogel was comparable to that of the original hydrogel ($\varepsilon' = \sim 280\%$, $f =$ 0.88–0.99). When [MBAA] was 0%, the absence of chemical cross-linking in the hydrogel generated a viscous hydrogel that was lacking mechanical properties. Although the healing efficiency of the purely ionic cross-linked hydrogel was ~0.99, the healing was mostly due to the viscosity of the gel. This observation confirms that chemical cross-linking is important for providing the hydrogel with mechanical strength to maintain its stability in shapes and architectures. Hydrogels with [MBAA] of 0.1% are stable and have a reasonably high healing efficiency. However, the self-healing properties of the samples decline

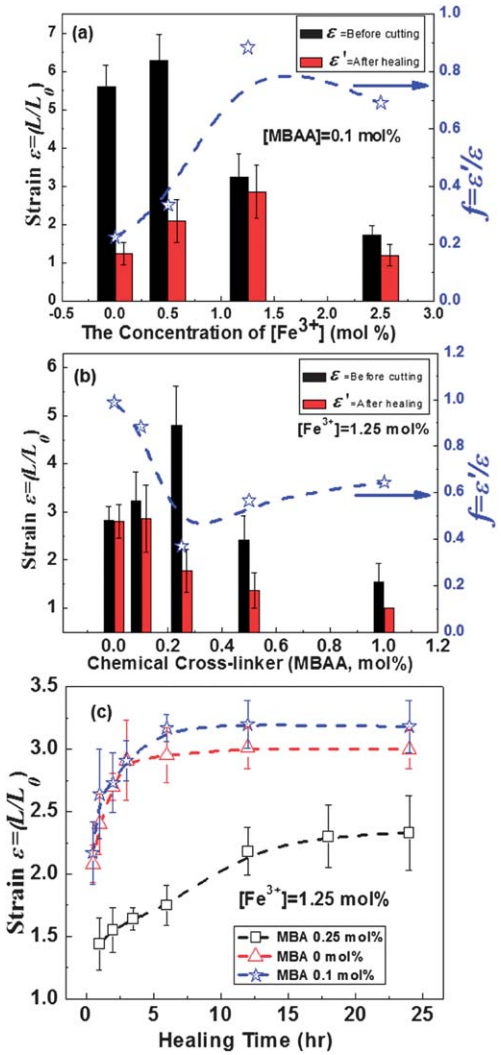

Fig. 4 The self-healing properties of the hydrogel. (a and b) Maximum strain of healed hydrogel (ε') and original hydrogels (ε) (left) and self-healing efficiency (f) (right) of the hydrogel as a function of the Fe^{3+} concentration at a constant MBAA concentration of 0.1% (a), and as a function of the MBAA concentration at a constant Fe^{3+} concentration of 1.25% (b). (c) The maximum strain of hydrogels with a constant Fe^{3+} concentration of 1.25 mol% and different MBAA concentrations as a function of self-healing time. The vertical error bars represent the standard deviation ($n = 3$).

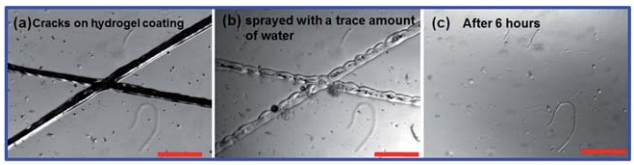

Fig. 5 The use of a dried self-healing hydrogel film as a protective coating. (a) A hydrogel coating with a crack of about 100 μm on a glass surface. (b) The hydrogel was sprayed with a trace amount of water. (c) The cracks self-healed completely after 6 hours. The scale bar is 500 μm.

drastically with the increase of [MBAA]. We presume that this can be explained by (i) a slow diffusion of metal ions at high cross-linking density of the hydrogel, and (ii) a reduced mobility of the PAA chain segments at a high density of covalent bonding. Fig. 4b shows that ε at 0.25% [MBAA] is larger than ε at 0% [MBAA]. This indicates that a low [MBAA] can enhance the elastic properties of the hydrogel, while a high [MBAA] (above 0.5%) results in a stiffer hydrogel matrix, and ultimately a decrease in elastic properties of the hydrogel. An optimal [MBAA] and Fe^{3+} can synergistically stabilize the hydrogel matrix, and increase its mechanical properties.

Finally, we studied the time dependency of the self-healing of the gel. Fig. 4c plots the ε' of the hydrogel as a function of healing time at various concentrations of MBAA. For hydrogels with a high [MBAA], the self-healing of hydrogels takes a much longer time due to the slow diffusion of Fe^{3+} and the reduced mobility of the segments of PAA chains. The hydrogel of 0% MBAA requires only about 4.5 hours to self-heal, as indicated by an approximately constant ε'. In contrast, the hydrogel of 0.25% MBAA needs about 20 hours to self-heal.

These PAA hydrogels can withstand and recover from a substantial amount of damage. To demonstrate the potential use of the hydrogel as a protective coating, we coated a glass slide with the self-healing hydrogel (Entry 3) (Fig. 5). After drying, the hydrogel formed a protective film on the substrate. The dried hydrogel coating was mechanically damaged to form cracks with a width of ~100 μm (Fig. 5a). Upon spraying a trace amount of water onto the surface, the cracks of the dried hydrogels self-healed after 6 hours (Fig. 5b and c). This coating can also self-heal under a moist environment without the intentional addition of water. Similar to the classic acrylate coating available in the business market, we are aware that these PAA-based hydrogels could adhere to various substrates such as silicon wafers, glass slides, wood board, concrete walls, metal, and even polystyrene surfaces, which may enable their potential use as protective coatings for a wide range of surfaces.

In summary, we have developed a facile yet versatile method to design self-healing hydrogels using the migration of metal ions and the mobility of polymer chains. The self-healing of the hydrogel is repeatable, and does not decay after many cycles of cutting and healing. We further demonstrated that the self-healing hydrogel can be used as a protective coating that is capable of repairing itself from mechanical damage. The self-healing hydrogel material may find applications in smart coatings, soft robots, and biomedical devices. However, a high concentration of Fe^{3+} may not be desirable in biomedical applications. A more detailed study of this for self-healing hydrogels will be investigated in future work.

This work is supported by the startup fund from the University of Maryland. Z.H. NIE thanks the support of the Research and Scholarship Award from the University of Maryland. C.Y. WANG thanks the support of the 973 Program (2012CB821500) and NSFC (21274046). Z.J. WEI thanks the support of China Scholarship Council.

Notes and references

1 J. P. Gong and W. Hong, *Soft Matter*, 2012, **8**, 8006–8007.
2 R. J. Russell, M. V. Pishko, C. C. Gefrides, M. J. McShane and G. L. Cote, *Anal. Chem.*, 1999, **71**, 3126–3132.

3 J. K. Oh, R. Drumright, D. J. Siegwart and K. Matyjaszewski, *Prog. Polym. Sci.*, 2008, **33**, 448–477.
4 J. He, X. Tong and Y. Zhao, *Macromolecules*, 2009, **42**, 4845–4852.
5 Y. L. Zhang, L. Tao, S. X. Li and Y. Wei, *Biomacromolecules*, 2011, **12**, 2894–2901.
6 A. Phadke, C. Zhang, B. Arman, C. C. Hsu, R. A. Mashelkar, A. K. Lele, M. J. Tauber, G. Arya and S. Varghese, *Proc. Natl. Acad. Sci. U. S. A.*, 2012, **109**, 4383–4388.
7 K. Wang, Q. Fu, W. F. Li, Y. Gao and J. Y. Zhang, *Polym. Chem.*, 2012, **3**, 1539–1545.
8 M. Otake, Y. Kagami, M. Inaba and H. Inoue, *Rob. Auton. Syst.*, 2002, **40**, 185–191.
9 G. H. Kwon, Y. Y. Choi, J. Y. Park, D. H. Woo, K. B. Lee, J. H. Kim and S. H. Lee, *Lab Chip*, 2010, **10**, 1604–1610.
10 R. Censi, P. Di Martino, T. Vermonden and W. E. Hennink, *J. Controlled Release*, 2012, **161**, 680–692.
11 T. A. Asoh, W. Kawai and A. Kikuchi, *Soft Matter*, 2012, **8**, 1923–1927.
12 H. D. Lu, M. B. Charati, I. L. Kim and J. A. Burdick, *Biomaterials*, 2012, **33**, 2145–2153.
13 B. Yang, Y. L. Zhang, X. Y. Zhang, L. Tao, S. X. Li and Y. Wei, *Polym. Chem.*, 2012, **3**, 3235–3238.
14 M. M. Zhang, D. H. Xu, X. Z. Yan, J. Z. Chen, S. Y. Dong, B. Zheng and F. H. Huang, *Angew. Chem., Int. Ed.*, 2012, **51**, 7011–7015.
15 J. Hentschel, A. M. Kushner, J. Ziller and Z. B. Guan, *Angew. Chem., Int. Ed.*, 2012, **51**, 10561–10565.
16 H. Ceylan, M. Urel, T. S. Erkal, A. B. Tekinay, A. Dana and M. O. Guler, *Adv. Funct. Mater.*, 2013, **23**, 2081–2090.
17 M. Burnworth, L. M. Tang, J. R. Kumpfer, A. J. Duncan, F. L. Beyer, G. L. Fiore, S. J. Rowan and C. Weder, *Nature*, 2011, **472**, 334–337.
18 L. Huang, N. Yi, Y. Wu, Y. Zhang, Q. Zhang, Y. Huang, Y. Ma and Y. Chen, *Adv. Mater.*, 2013, **25**, 2224–2228.
19 M. Nakahata, Y. Takashima, H. Yamaguchi and A. Harada, *Nat. Commun.*, 2011, **2**, 511.
20 T. Kakuta, Y. Takashima, M. Nakahata, M. Otsubo, H. Yamaguchi and A. Harada, *Adv. Mater.*, 2013, **25**, 2849–2853.
21 H. Zhang, H. Xia and Y. Zhao, *ACS Macro Lett.*, 2012, **1**, 1233–1236.
22 Y. L. Zhang, B. Yang, X. Y. Zhang, L. X. Xu, L. Tao, S. X. Li and Y. Wei, *Chem. Commun.*, 2012, **48**, 9305–9307.
23 P. Mukhopadhyay, N. Fujita, A. Takada, T. Kishida, M. Shirakawa and S. Shinkai, *Angew. Chem., Int. Ed.*, 2010, **49**, 6338–6342.
24 Y. L. Chen, A. M. Kushner, G. A. Williams and Z. B. Guan, *Nat. Chem.*, 2012, **4**, 467–472.
25 J. Y. Sun, X. H. Zhao, W. R. K. Illeperuma, O. Chaudhuri, K. H. Oh, D. J. Mooney, J. J. Vlassak and Z. G. Suo, *Nature*, 2012, **489**, 133–136.
26 S. R. White, N. R. Sottos, P. H. Geubelle, J. S. Moore, M. R. Kessler, S. R. Sriram, E. N. Brown and S. Viswanathan, *Nature*, 2001, **409**, 794–797.
27 A. B. W. Brochu, S. L. Craig and W. M. Reichert, *J. Biomed. Mater. Res., Part A*, 2011, **96A**, 492–506.
28 B. J. Blaiszik, S. L. B. Kramer, S. C. Olugebefola, J. S. Moore, N. R. Sottos and S. R. White, *Annu. Rev. Mater. Res.*, 2010, **40**, 179–211.
29 F. Peng, G. Z. Li, X. X. Liu, S. Z. Wu and Z. Tong, *J. Am. Chem. Soc.*, 2008, **130**, 16166–16167.